Development of a Linearly Responsive Electromagnetic Actuator

Chih-Hung G. Li, and Hiep Phuong Nguyen

***Abstract*—**A novel electromagnetic actuator is reported in this paper. The device can be used as a precision position provider, as the movement of the free solenoid responds linearly to the input electric current. Such a linear relationship can make it very easy to control the device, with a simple open-loop control scheme. The novel actuator comprises of two solenoids and an elastomeric cone, sandwiched in between the solenoids. The elastomeric cone provides non-linear reaction force in resistance to the electromagnetic force, and as a result, force equilibrium can be achieved at the desired working points to form a straight line of position response versus input current. Finite element analysis was used for accurate calculation of the highly non-linear spring characteristics of the elastomeric cone. Among the geometries studied, it was found that a cone shape of 6mm in height, 7mm in diameter, and an aperture of 57^o produces a force-displacement curve that best suits the need for the spring performance. A prototype of the actuator, along with the elastomeric cone was made and tested. The results showed that the movement of the actuator responds to the input current quite linearly, with an R^2 of 0.983.

***Keywords*—**Actuator, artificial muscle, finite element, pull-in

I. Introduction

ELECTROMAGNETIC solenoid is a common type of electromagnet for the purpose of generating a controlled magnetic field. It is widely applied in industry as, for example, a solenoid switch, which is a specific type of relay that operates an electrical switch. The operating principle is quite simple. As the electric current flows through the solenoid, a magnetic force is generated, and the movable iron armature is attracted by the electromagnet to switch on an electric circuit. When the electric current ceases to flow through the solenoid, the magnetic force disappears, the armature bounces back with the help of a spring, and the electric circuit can be switched off [1]. By adapting this simple principle, Lu and others demonstrated a design of inchworm mobile robot using the electromagnetic linear actuator [1]. A gripping device with compliant mechanism and planar moving coil actuator was also created [2]. As electromagnetic actuator features moderate output force, large displacement, and can be driven by common low cost, low voltage controller, it has good potential of being a precision motion or position provider [3]-[4], in which the force equilibrium is involved between the electromagnetic force and an elastic load. However, one major difficulty with the solenoid is the highly non-linear nature of the electromagnetic force with respect to the air gap and the electric current. Since the electromagnetic force of a solenoid is approximately proportional to the square of the current and inversely proportional to the square of the distance of the air gap, the force increases dramatically when the air gap is closing up. In other words, when the armature moves toward the solenoid, the attractive force increases non-linearly, and soon it becomes extremely difficult to achieve force equilibrium. From a force equilibrium point of view, when the electric current is increased working against a linear elastic load, the working point responds to the electric current non-linearly, making it extremely difficult to control the position precisely [5]. Similar difficulty is also seen in electrostatic actuators, where the well-known pull-in effect can cause an electrostatically actuated beam or diaphragm to collapse on the ground plane if the drive voltage exceeds certain limit [6]-[8]. Thus, for precise position control of the solenoid actuator, sophisticated control algorithm needs be developed. For example, an extended state observer-based time-optimal control is proposed for fast and precise point-to-point motions driven by a novel electromagnetic linear actuator [9]. In an application for precise valve position control, a direct adaptive non-linear control framework is presented [10]. However, for many applications, the control scheme can be much easier, if the actuator is designed in a way that the movement of the moving armature responds proportionally to the input voltage or current in a linear fashion. However, as the working point is determined by the force equilibrium between the electromagnetic force and the elastic load, a conventional linearly responsive spring will not be able to accomplish this task [5]. Therefore, we propose here to develop a new type of electromagnet actuator incorporating a non-linear elastic component in order to provide the linearly proportional position response mentioned above. To do this, an elastomeric cone is proposed for the non-linear elastic component. The elastomeric cone will provide non-linear reaction force in resistance to the electromagnetic force, and as a result, force equilibrium can be achieved at the desired working points to form a straight line of position response versus input current.

In general, the new electromagnetic actuator proposed here is expected to have the following advantages:

i. Low noise: As automated equipment often uses step motors as the motion provider, the noise associated with it is often annoying. The concept proposed here can be much quieter, since no metal contact exists in the proposed design.

Chih-Hung G. Li is with the Minghsin University of Science and Technology, Department of Mechanical Engineering, No.1, Xinxing Rd., Xinfeng Hsinchu 30401, Taiwan(R.O.C) (corresponding author's phone: 03-559-3142 ; e-mail:cL4e@must.edu.tw).

Hiep Phuong Nguyen, was with Minghsin University of Science and Technology, Department of Mechanical Engineering, No.1, Xinxing Rd., Xinfeng Hsinchu 30401, Taiwan(R.O.C).

ii. Easy control: Since the movement of the actuator responds to the input current linearly, the control scheme for a complex motion sequence can be easily formulated with a simple open-loop controller.
iii. Slender form: Multiple units of the proposed actuator can be connected in series to form a slender motion provider for greater movement. It will be particularly suitable for applications in a limited narrow space.
iv. Low vibration: The elastomeric spring between the solenoids can serve as a damper to absorb vibration. And unlike a step motor relying on pulse inputs, the continuous input greatly reduces the possibility of vibration.
v. Ease of extension to applications of multi-degrees of freedom: As the structure of the actuator is very simple, it is easy to combine units of actuators in different directions to provide motions of multi-degrees of freedom.

In this paper, the process of creating a linearly responsive electromagnetic actuator is reported. The process is illustrated in Fig. 1. To begin the design process, the ideal linear relationship between the input current and the motion provided must be decided. The nonlinear electromagnetic force as a function of input current and air gap must be determined first. By mapping the electric current-motion relationship on the force-air gap diagram and working out the force equilibrium, the ideal force-displacement relationship for the elastic component can be obtained. To acquire an elastic component with the ideal non-linear force-displacement characteristics, an elastomeric cone is devised; the spring characteristics are calculated using nonlinear finite element analysis. When the shape, the dimensions, and the elastic properties of the elastomeric cone are confirmed in the FEA to provide the desired performance, a prototype of the actuator with the elastomeric cone can be made. The performance of the proposed actuator is then measured to check with the previously defined linear current-motion requirement.

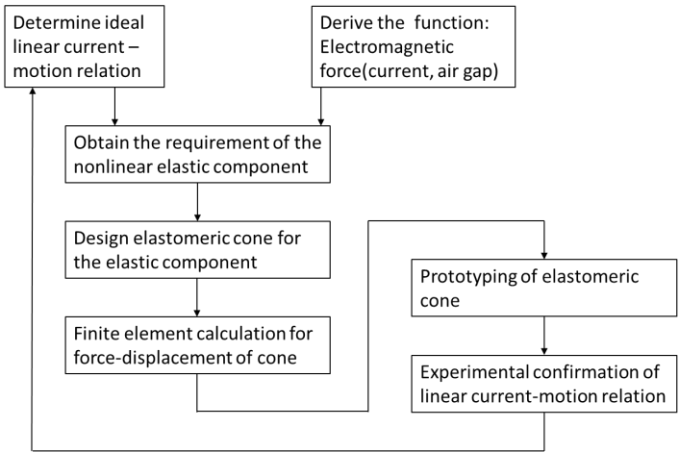

Fig. 1 Schematic of the development process of the linearly responsive electromagnetic actuator

II. Design of the Linearly Responsive Electromagnetic Actuator

The proposed design consists of two electromagnets and an elastomeric spring as shown in Fig. 2(a) [11]. The electromagnet includes a cylindrical steel core and a copper wire rounding the steel core as depicted in Fig. 2(b). The elastomeric spring is proposed to be cone-shaped, so the reaction force it generates will increase non-linearly while being compressed by the electromagnets. When the electric current of the same direction is supplied to both electromagnets, the electromagnets will generate an attractive force to attract one another. The attractive force compresses the elastomeric spring until force equilibrium between the electromagnetic attraction and the elastomeric resistance has been achieved. Since the air gap between the two electromagnets is determined by the force equilibrium between the electromagnetic force and the spring resistance, by increasing the input current, the air gap can be reduced, and the free electromagnet will move accordingly. By connecting multiple units in series as shown in Fig. 3, greater movement can be achieved, and the actuators can perform like an artificial muscle.

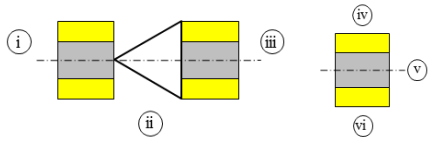

Fig. 2 The proposed linearly responsive actuator: (a) A single unit of the actuator with a cone-shaped elastomeric spring; (i) and (iii) are two electromagnets; (ii) is the elastomeric spring, (b) The electromagnet; (iv) and (vi)represent the copper wire; (v) is the steel core.

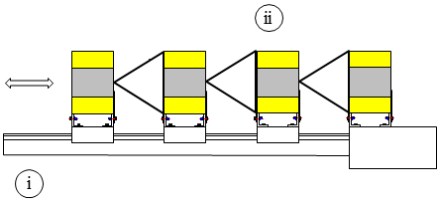

Fig. 3 A schematic of series of linearly responsive actuators for greater movement; (i) the guide rail, (ii) units of the actuator.

The advantage of using a nonlinear spring as shown in Fig. 4(b) in replacement of a conventional linear spring as shown in Fig. 4(a) is explained by Fig. 5, where the force-displacement relationships of the electromagnetic forces and the force characteristics of springs are displayed together. The multiple solid lines represent the electromagnetic forces associated with various levels of electric current and air gap. For a conventional linear spring, the force-displacement relationship is the bi-linear line as shown in Fig. 5(a). When the linear spring is functioning within the normal range, the force-displacement relation is a straight line with a desired constant slope, which is the spring stiffness. When the spring is compressed to a point that contact between the coils has happened, the spring will become extremely stiff and the system can no longer properly function. The nearly vertical section of the bi-linear lines demonstrates such a scenario. However, for the elastomeric cone, the hyperelastic behavior of the material along with a

proper shape makes it possible to generate a reaction force that increases highly nonlinearly as shown in Fig. 5(b) [12].

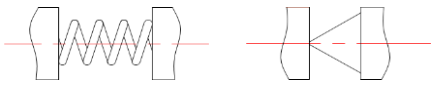

(a) (b)

Fig. 4 Comparison of linear and non-linear springs: (a) A conventional coil spring, (b) An elastomeric cone.

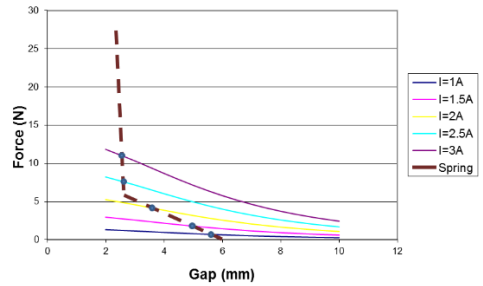

(a)

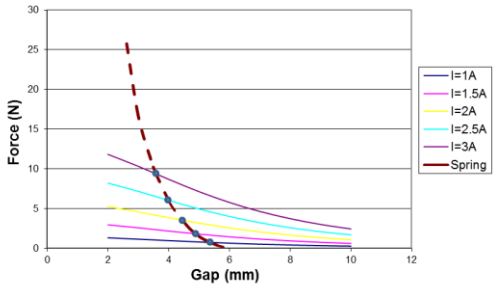

(b)

Fig. 5 Diagrams of spring force and electromagnetic force: (a) Bilinear force-displacement relationship of a conventional linear spring, (b) Nonlinear force-displacement relationship of the desired spring characteristics.

In Fig. 5, the intersection point between the electromagnetic force and the spring force represents the force equilibrium associated with every electric current input. The corresponding air gap between the two electromagnets also represents the position of the free electromagnet, revealing the distance it moves before equilibrium is achieved. If one plots all of these intersection points in a diagram of displacement vs. current, the performance characteristics of the two systems can be compared, as shown in Fig. 6. For an example of the linearly responsive spring as shown in Fig. 6(a), the relationship between actuator displacement and input current is clearly not linear. For electric current inputs between 1.5 A and 2.2 A, the displacement increases acceleratingly with input current. For electric currents above 2.2 A, the device does not function anymore, as the motion has reached its limit. In contrast, for a desired nonlinearly responsive spring as shown in Fig. 6(b), the actuator displacement appears quite linear with respect to the input current. Not only the operable range is greatly extended, but also the motion control can be much easier.

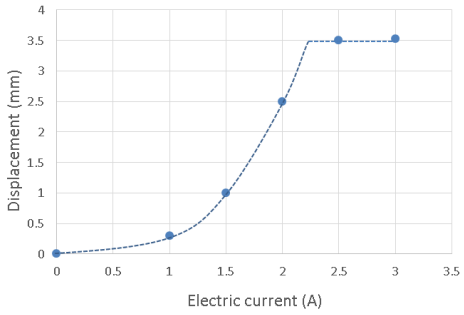

(a)

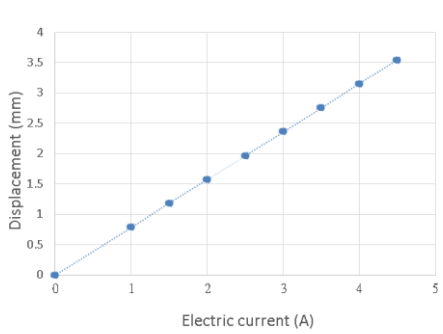

(b)

Fig. 6 Diagrams of actuator displacement vs. electric current input: (a) Using a conventional linearly responsive spring; (b) Using an ideal nonlinearly responsive spring.

To obtain the electromagnetic force as a function of electric current and air gap, measurement was performed. An apparatus was designed to measure the electromagnetic forces associated with various air gaps and electric currents (see Fig. 7). Electromagnets are prepared with an iron core of a radius R= 7mm, a core length L= 30mm, and 480 turns of copper wire around the core. One of the electromagnets is fixed directly to the apparatus, and the other one is connected to a force gauge fixed on the apparatus, with a prescribed air gap between the two electromagnets. A power supply is used to provide the same electric current to the electromagnets; an attractive force is generated and measured by the force gauge. By adjusting the position of the fixed electromagnet, the air gap can be adjusted. The attractive force between the electromagnets is measured as a function of gap distance and electric current. The results are shown in Fig. 8.

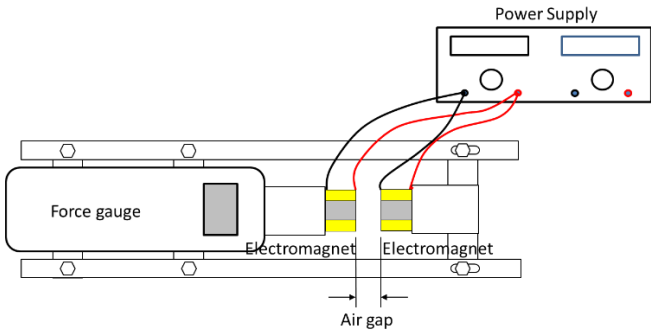

Fig. 7 Schematic of the apparatus for measurement of the electromagnetic force

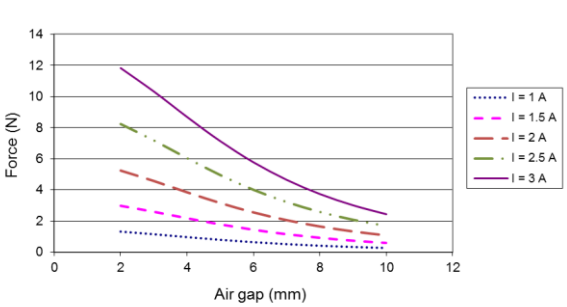

Fig. 8 The electromagnetic attraction between solenoids as a function of air gap for various input currents.

III. Finite Element Analysis

As discussed in Section 2, in order to create a linearly responsive actuator as shown in Fig. 6(b), the elastomeric spring must possess highly nonlinear spring characteristics providing a rapidly increasing spring rate to balance the rapidly increasing electromagnetic force. To achieve this, we propose a conical shape for the elastomeric spring as shown in Fig. 9. The cone has two end areas, one relatively larger than the other. When the cone is barely compressed, the initial stiffness is low since the cross-sectional area of the small end is small, and the compressive displacement associated with the smaller end is greater. When compression progresses, side areas of the cone near the small end will gradually move into contact with the compressing component; so the true contact area of the small end becomes significantly larger. As a result, the small end actually becomes a much larger end, and the stiffness of the cone can become effectively higher. The material non-linearity also progresses in a similar fashion, as the elastic modulus becomes higher at higher strains [13]. From Fig 5(b), we have derived the requirement on the force-displacement relationship of the desired elastomeric spring, whose spring characteristics strongly depend on its own geometry [14]. In general, a cone can be defined by a base diameter *D*, and an aperture θ. For stability, we devise a small area on the top of the cone, instead of a point. In general, the diameter of the top area is less than 1/10 of the base diameter. Hence, the height *h* is slightly smaller than that of a perfect cone as shown in Fig. 9.

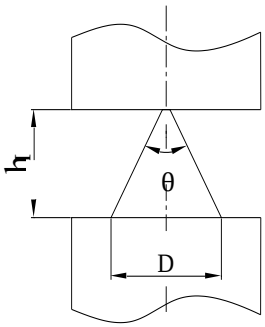

Fig. 9 Proposed conical shape of the elastomeric spring.

The geometric parameters of the elastomeric cone in Fig. 9 must be judiciously determined in order to obtain the required non-linear spring characteristics shown in Fig. 6(b). To calculate the force-compression relationship of the cone, we use finite element analysis to perform a series of structural analyses. In each analysis, the force-displacement curve is obtained for a given set of geometric parameters. The set of geometric parameters associated with the best curve fitting is to be found. The finite element models involve a Hyper-Elastic material model, large strain, and contact. Finite element software ANSYS 10.0 was used for the calculation with the non-linear solution procedure activated [15]. In ANSYS, many Hyper-Elastic material models are available including Mooney-Rivlin, Polynomial, Yeoh, Neo-Hookean, Ogden, Arruda-Boyce, Gent, Blatz-Ko, and Ogden Hyper-Foam. In the current study, the Neo-Hookean material law is used for its simplicity and ease to be directly linked to the Young's Modulus. The strain energy function of the Neo-Hookean model is:

$$W = C_1(I_1 - 3) + d(J - 1)^2, \quad (1)$$

where *W* is the strain energy function, C_1 equals to a half of the initial shear modulus of elasticity. And $d = 2/K$, where *K* is the initial bulk modulus. I_1represents the first invariant of the deformation tensor as,

$$I_1 = \bar{\lambda}_1^{\,2} + \bar{\lambda}_2^{\,2} + \bar{\lambda}_3^{\,2} \quad (2)$$

where $\bar{\lambda}_i$denotes the principal stretch ratio in each direction. In addition,

$$J = \bar{\lambda}_1\bar{\lambda}_2\bar{\lambda}_3 \quad (3)$$

The Neo-Hookean model in ANSYS permits to specify absolute incompressibility for the material. Hence, *d* is set to be zero, and C_1 is set at 0.4167 MPa based on an initial Young's Modulus of 2.5 MPa. Since the shape of the cone and the compressive loading are axi-symmetric, the three-dimensional problem can be simplified to be an axi-symmetric finite element model with plane elements as shown in Fig. 10.

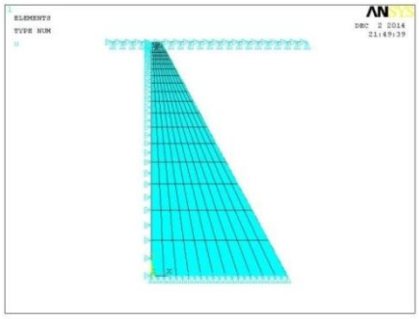

Fig. 10 The axi-symmetric finite element model of the conical elastomeric spring

The elastomer domain of the finite element model is meshed with an 8-noded element type PLANE183. The contact interaction is modeled with the contact element type TARGE169 and CONTA172 as shown in Fig. 11, in which the boundary of the cone is meshed with soft contact element CONTA172 (deformable), and a straight line on top of the small end representing the rigid compressive component is meshed with rigid contact element TARGE169 (non-deformable). As the compressive component moves downward relatively, compression is imposed on the elastomer. The side areas of the cone gradually move into contact with the rigid component on the top. Since the entire side areas of the cone are meshed with contact elements, it is guaranteed that the

contact interaction between the compressive component and the cone is properly simulated.

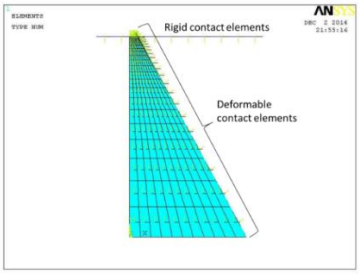

Fig. 11 Contact elements of the finite element model

To simulate the compression process, the rigid line at the top is fully constrained; the bottom line of the elastomeric cone is specified to be rigid and move upward by a maximum displacement of 3.4 mm, which matches a compression ratio of 57%. Since the element deformation is high and the contact elements are used in the model, the large deformation option in the ANSYS solution procedure is activated. The entire loading process is divided into 13 load steps, and each load step is divided into 5,000 sub-steps for solution accuracy. The option of automatic step size is also activated with the minimum step number set at 100, and the maximum step number set at 20,000. Some typical calculation results of the deformed plots are shown in Fig. 12.

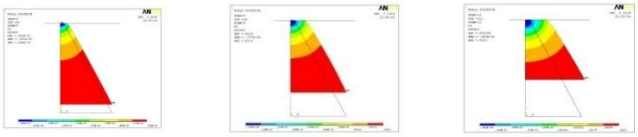

(a) (b) (c)

Fig. 12 FEA results at various compression ratios: (a) 10%, (b) 25%, and (c) 38%

Among the geometries analyzed in ANSYS (see Fig. 13), it is found that in model I with h = 6mm, D = 7mm, and $\theta = 57^o$, the solution reveals the best fit for Fig. 5(b). The calculated force-displacement relationship is shown in Fig. 14(a) in comparison with the theoretical requirements. Non-dimensionalized forces with respect to the Young's modulus and the base area are also shown in Fig. 14(b) as a function of compression ratio. By plotting the above results on the diagram of the electromagnetic forces (see Fig. 8) and working out the intersections at each electric current like Fig. 5(b), the movement vs. current of the actuator can be predicted as shown in Fig. 15. It is found that the relationship is quite linear with a $R^2 = 0.992$.

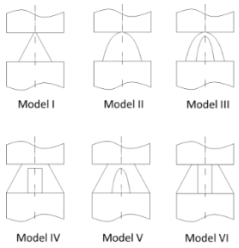

Fig. 13 Geometries tested in ANSYS for spring performance

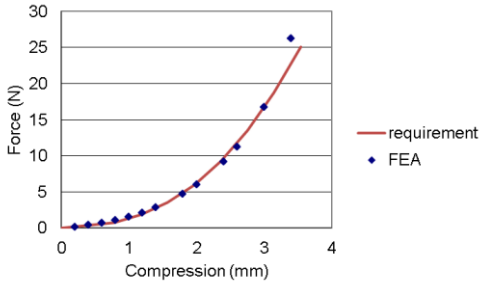

(a)

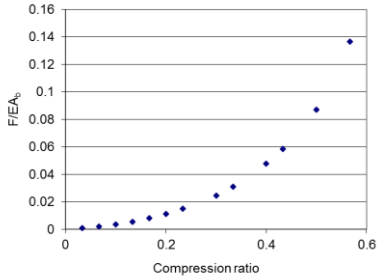

(b)

Fig. 14 The calculated spring characteristics for h = 6mm, D = 7mm, and $\theta = 57^o$ in comparison with the theoretical requirements: (a) Force vs. compression, (b) Non-dimensional results.

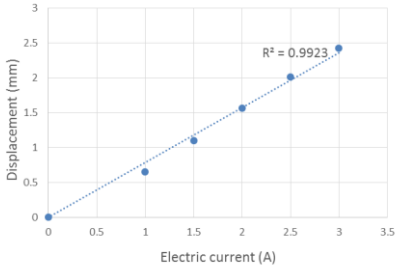

Fig. 15 Predicted performance of the linearly responsive actuator

IV. Prototype and Measurement

A prototype of the proposed electromagnetic actuator was built and tested. The actuator includes two major parts, an elastomeric spring and a pair of electromagnetic solenoids. The elastomeric spring was made according to the previous geometric parameters calculated in FEA and found to best fit the requirement for its non-linear requirement. To fabricate the elastomeric spring, the compression molding method was used, and a steel mold was made. An industrial grade NBR compound with a hardness of Shore A 50 degrees was chosen as the material [16]. NBR is a widely used compound, known for its low cost, high rebound capability, and high tear strength. Its excellent resistance to compression set is particularly suitable for our need, as the elastomeric cone is expected to be frequently under compression. The initial Young's modulus of the elastomer was measured to be 2.5 MPa, based on a simple extension test with a long rectangular specimen. A hydraulic press was used to compress the mold with a pressure of 80 kg/cm^2 and a curing temperature set at 170^{o}C. The cured elastomeric spring was then glued to one of the electromagnet as shown in Fig. 16(b).

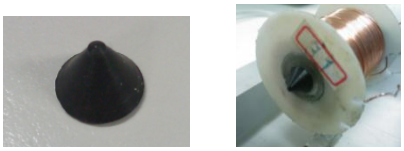

(a) (b)

Fig. 16 The prototype of the actuator: (a) The elastomeric cone, (b) The solenoid with the elastomeric cone.

A testing apparatus was then built, and the prototype of the proposed actuator was assembled as shown in Fig. 17. One electromagnet is fixed to the apparatus, and the other one is mounted on a linear slider, which is guided to move freely along the axial direction with minimal friction. The elastomeric spring glued to one of the electromagnets is placed in between them. A position sensor (LVDT) is used to detect the position of the free electromagnet; the measurement can also indicate the compression distance of the elastomeric spring. A power supply is used to input electric current to the solenoids in series. Five different levels of electric current were input for the test (see Table I). For each level of the input electric current, the free solenoid would be attracted by the other solenoid, and move to compress the elastomeric spring until force equilibrium was achieved. At least 3 seconds was waited, before every measurement of displacement was recorded. The recorded displacements of the free solenoid with respect to the input electric currents are shown in Table I.

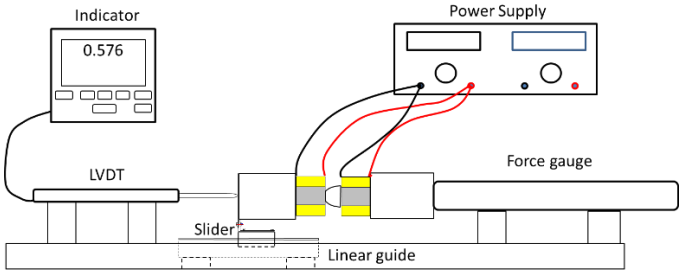

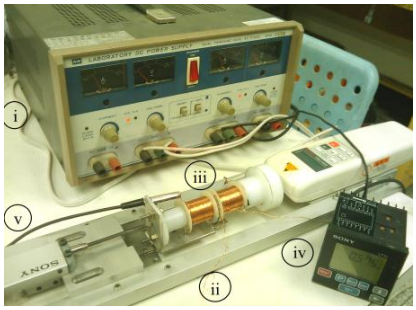

Fig. 17 The testing of the linearly responsive actuator; (i) the power supply, (ii) the fixture, (iii)the actuator being tested, (iv) the indicator of LVDT, and (v) the LVDT.

In Table I, *I* denotes the electric current input by the power supply, $d_{measured}$ is the measured movement of the free electromagnet, $d_{predicted}$ is the predicted movement, and Δd is the discrepancy between the two values. In general, the discrepancy is less than 5%, with a greatest of 10.8% at *I* = 1*A*. It is probably due to the fact that the Coulomb friction of the linear slider becomes relatively more important, when the electromagnetic force is low. Photographs of the actuator under various input currents are shown in Fig. 18. In Fig. 19 where both the measured and predicted displacements are plotted, it can be seen that the measured movement of the actuator also responds to the input current quite linearly. By fitting the measured data with a straight line, R^2 is found to be 0.983.

TABLE I
COMPARISON OF MEASURED AND PREDICTED DISPLACEMENTS VERSUS INPUT ELECTRIC CURRENTS

I (A)	$d_{measured}$ (mm)	$d_{predicted}$ (mm)	Δd (mm)	%Δd (%)
0	0	0	0	0
1	0.58	0.65	0.07	10.8
1.5	1.05	1.10	0.05	4.55
2	1.52	1.56	0.04	2.56
2.5	2.01	2.01	0.00	0.00
3	2.44	2.42	-0.02	-0.80

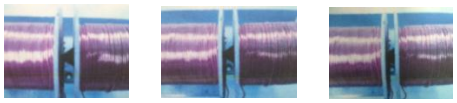

(a) *I* = 1A (b) *I* = 1.5A (c) *I* = 2A

(d) *I* = 2.5 A (e) *I* = 3 A

Fig. 18 Photographs of the actuator under various input currents.

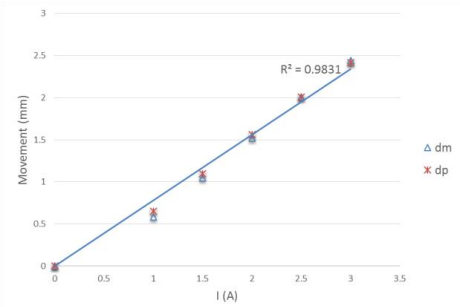

Fig. 19 Comparison of measured and predicted displacements versus electric current, dm: measurements; dp: predictions.

V. DISCUSSION

The results shown in Fig. 19 confirm the design concept proposed in this paper for creating a linearly responsive actuator. Although the R^2 of the measured data fitted to a straight line is found to be 0.983, discrepancies do exist compared with a perfect straight line. To further improve the linearity of the actuator performance, it is suggested that the shape of the conical elastomeric spring can be further fine-tuned. For example, by dividing the cone into certain sections, each with a prescribed cross-sectional diameter, the spring characteristics of the cone may be tweaked to better fit a straight line [14]. With the help of finite element analysis, models of various geometries can be swiftly examined to find a better shape of cone. For the prototype demonstrated in the current study, the largest displacement of the actuator ever reached is 2.42mm. The total length of the proposed actuator is:

$$L = 2L_{electromagnets} + L_{spring} = 66 \text{ mm}. \quad (4)$$

Hence, the contraction ratio of the proposed actuator, defined as the largest displacement divided by the total length of the device is computed to be 2.44/66 = 3.70%. The contraction ratio can be further improved, if the attractive force per length of the electromagnet is reduced. As the attractive force depends on the permeability and the diameter of the core, the ratio of force per volume can be greatly enhanced by using a material with a higher permeability. The electromagnetic cores used in the current study are made of steel, which has a permeability μ around $3x10^{-4}$(H/m). Materials with higher permeability such as Permalloy can be one good choice. Commercial Permalloy alloys typically have relative permeability of around 100,000, compared to several thousand for ordinary steel [17]. Thus, by using Permalloy, it is expected to shorten the electromagnets of the actuator by at least 10 times, making a contraction ratio of approximately 20%. For an application resembling an artificial muscle combining multiple units of the actuators in series, the contraction ratio can be further increased. For example, a device with 10 solenoids and 9 elastomeric cones will present a contraction ratio of 26%. Such a contraction ratio makes it comparable to many of the existing artificial muscles, and superior to many others. For example, shape memory alloys SMAs reportedly generate a contraction of 3% [18]. Piezoelectric materials PZTs offer low strains (~0.06%) with significant hysteresis (~15–20%), where as electrostrictive PMN materials exhibit higher strains (~0.1%) with lower hysteresis (~1–4%) [19]. Pneumatic muscle actuator (PMA), in general, exhibits a contraction ratio of 25% [20]. Dielectric elastomers are reported to associate a maximum contraction ratio of 32 %; however, the high voltage needed for operation presents a main disadvantage [21].

VI. Conclusion

We have proposed a novel design of electromagnetic actuator, whose displacement responds linearly to the input electric current. The proposed design contains two electromagnetic solenoids and an elastomeric cone, sandwiched in between the solenoids. The nonlinear spring force of the elastomeric cone is customized to accurately balance the nonlinear electromagnetic force at each desired input level of the electric current. To design the ideal elastomeric cone, a few geometries were tested. Finite element analysis was used for accurate calculation of the force-displacement relationship of the cone. The nonlinear finite element models involved Neo-Hookean material law and contact elements. Among the geometries studied, it was found that a cone shape of 6mm in height, 7mmin diameter, and an aperture of 57^o generates a spring curve that best suits the need. A prototype of the actuator was made, with the elastomeric cone made of an industrial grade NBR. The performance of the actuator was tested by measuring the motion response at every input current. The results showed that the movement of the actuator responds to the input current quite linearly, with an R^2 of 0.983.

Acknowledgment

The author is grateful for the research funding from the Central Taiwan Science Park of the National Science Council of Taiwan (ROC) under the account number of 30120210.

References

[1] H. Lu, J. Zhu, Z. Lin, Y. Guo, "An inchworm mobile robot using electromagnetic linear actuator," *Mechatronics*, vol. 19, pp. 1116–1125, 2009.
http://dx.doi.org/10.1016/j.mechatronics.2008.07.009

[2] E. Kallenbacha, H. Kube, V. Zoppig, K. Feindt, R. Hermann, F. Beyer, "New polarized electromagnetic actuators as integrated mechatronic components – design and application," *Mechatronics*, vol. 9, pp. 769-784, 1999.
http://dx.doi.org/10.1016/S0957-4158(99)00029-X

[3] I. M. Chen, M. E. H. Benbouzid, H. Ding, W. J. Kim, C. H. Menq, "Guest Editorial Introduction to the Focused Section on Electromagnetic Devices for Precision Engineering," *IEEE/ASME Trans on Mechatron*, vol. 16, pp. 401-410, 2011.
http://dx.doi.org/10.1109/TMECH.2011.2131147

[4] O. Chaides, H. Ahuett-Garza, "Design and characterization of a linear micropositioner based on solenoid and compliant mechanism," *Mechatronics*, vol. 21, pp. 1252–1258, 2011.
http://dx.doi.org/10.1016/j.mechatronics.2011.08.005

[5] O. Gomis-Bellmunt, S. Galceran-Arellano, A. Sudria`-Andreu, D. Montesinos-Miracle, L. F. Campanile, "Linear electromagnetic actuator modeling for optimization of mechatronic and adaptronic systems," *Mechatronics*, vol. 17, pp. 153–163, 2007.
http://dx.doi.org/10.1016/j.mechatronics.2006.07.002

[6] S. Chowdhury, M. Ahmadi, W. C. Miller, "A closed-form model for the pull-in voltage of electrostatically actuated cantilever beams," *J Micromech Microeng*, vol. 15, pp. 756-763, 2005
http://dx.doi.org/10.1088/0960-1317/15/4/012.

[7] R. Puers, D. Lapadatu, "Electrostatic forces and their effects on capacitive mechanical sensors," *Sensors and Actuators A*, vol. 56, pp. 203–210, 1996.
http://dx.doi.org/10.1016/S0924-4247(96)01310-6

[8] S. Chowdhury, M. Ahmadi, W. C. Miller, "A comparison of pull-in voltage calculation methods for MEMS-based electrostatic actuator design," *1st Int Conf on Sens Technol Novemb 21-23*, Palmerst N, N Z; 2005.

[9] X. Shi, S. Chang, "Extended state observer-based time-optimal control for fast and precise point-to-point motions driven by a novel electromagnetic linear actuator," *Mechatronics*, vol. 23, pp. 445–451, 2013.
http://dx.doi.org/10.1016/j.mechatronics.2013.03.007

[10] P. Mercorelli, "A Lyapunov-based adaptive control law for an electromagnetic actuator," *AASRI Procedia*, vol. 4, pp. 96-103, 2013.
http://dx.doi.org/10.1016/j.aasri.2013.10.016

[11] C. G. Li, "Electromagnetic actuator structure," Republic of China patent number I458250, October 2014.

[12] S. D. Noble, A. T. Dudding, C. W. Forrest, M. Brannigan, J. W. Stuart, M. P. Robinson, "Elastomeric Spring Vehicle Suspension," US patent number 7926836, 2011.

[13] O. H. Yeoh, "Characterization of elastic properties of carbon-black-filled rubber vulcanizates," *Rubber Chem Technol*, vol. 63, pp. 792-805, 1990.
http://dx.doi.org/10.5254/1.3538289

[14] C. G. Li, "A novel suspension strut featuring constant resonance frequency," *Int J Heavy Veh Syst*, to be published.

[15] *ANSYS ED User's Manual 10.0*. Pennsylvania : ANSYS Inc, 2005.

[16] A. N. Gent, "On the relation between indentation hardness and Young's modulus," *Inst Rubber Ind-Trans*, vol. 34, pp. 46–57, 1958.
http://dx.doi.org/10.5254/1.3542351

[17] P. Ciureanu, S. Middelhoek, *Thin Film Resistive Sensors*. London: Institute of Physics Publishing, 1992.

[18] D. Reynaerts, H. Van Brussel, "Design aspects of shape memory actuators," *Mechatronics*, vol. 8, pp. 635–656, 1998.
http://dx.doi.org/10.1016/S0957-4158(98)00023-3

[19] A. Suleman, S. Burns, D. Waechter, "Design and modeling of an electrostrictive inchworm actuator," *Mechatronics*, vol. 14, pp. 567–586, 2004.
http://dx.doi.org/10.1016/j.mechatronics.2003.10.007

[20] J. F. Zhang, C. J. Yang, Y. Chen, Y. Zhang, Y. M. Dong, "Modeling and control of a curved pneumatic muscle actuator for wearable elbow exoskeleton," *Mechatronics*, vol. 18, pp. 448–457, 2008. http://dx.doi.org/10.1016/j.mechatronics.2008.02.006

[21] R. Pelrine, R. Kornbluh, J. Joseph, R. Heydt, Q. Pei, S. Chiba, "High-field deformation of elastomeric dielectrics for actuators," *Mater Sci Eng C*, vol. 11, pp. 89-100, 2000. http://dx.doi.org/10.1016/S0928-4931(00)00128-4